J Control Theory Appl 2012 10 (4) 426–434
DOI 10.1007/s11768-012-0319-0

Vehicle adaptive cruise control design with optimal switching between throttle and brake

Lihua LUO [1], Ping LI [2], Hui WANG [2]

1.College of Transport and Communication, Shanghai Maritime University, Shanghai 200135, China;

2.State Key Laboratory of Industrial Control Technology, Zhejiang University, Hangzhou Zhejiang 310027, China

Abstract: For vehicle adaptive cruise control (ACC) systems, the switching performance between throttle and brake determines the driving comfort, fuel consumption and service lives of vehicle mechanical components. In this paper, an ACC algorithm with the optimal switching control between throttle and brake is designed in model predictive control (MPC) framework. By introducing the binary integer variables, the dynamics of throttle and brake are integrated in one model expression for the controller design. Then the ACC algorithm is designed to satisfy not only safe car following, but also the optimal switching between throttle and brake, which leads to an online mixed integer quadratic programming solved by the nested two-loop method. The simulation results show that the proposed ACC algorithm meets the requirements of safe car following, outperforms the traditional algorithms by performing smoother responses, reducing the switching times between throttle and brake, and therefore improves driving comfort and fuel efficiency significantly.

Keywords: Adaptive cruise control; Model predictive control; Optimal switching; Throttle; Brake

1 Introduction

Advanced driver assistant (ADA) systems are introduced to relieve human drivers from routine tasks, increase drivers' safety and comfort, reduce fuel consumption, and improve freeway capacity. Examples of ADA systems are adaptive cruise control (ACC) systems, Lane-Keeping systems, collision avoidance (CA) systems, and etc. [1–3].

An ACC vehicle adjusts its speed at a predefined value when there is no preceding vehicle. When a preceding vehicle is detected in the same lane, it automatically follows the preceding vehicle with a desired spacing. The control architecture for an ACC system is usually designed to be hierarchical and consists of two controllers [3]: the upper level controller determines the desired acceleration to satisfy the requirements based on measured signals; and the lower level controller activates the corresponding actuator (throttle or brake) according to the desired acceleration from the upper level controller. In the lower level controller, the switching strategy between throttle and brake is traditionally based on the simple threshold criteria [4–6]: if the desired acceleration from the upper level controller is larger than a critical value, the throttle is activated, or the brake is activated. While in [7], the switching rule is determined according to the current traffic situation, which will cause that the switching is sensitive to the surrounding traffic condition. Moreover, researchers have proposed a switching criterion by calculating the throttle and brake laws simultaneously and judging the corresponding sign of two control laws [8]. Above all, it can be seen that the switching control between throttle and brake is not fully considered in the procedure of ACC algorithm design, which may cause frequent switching, and thus lead to uncomfortable driving, increased fuel consumption and mechanical abrasion of vehicle components.

In this paper, an ACC algorithm with the optimal switching between throttle and brake is designed in model predictive control (MPC) framework. Song's longitudinal vehicle model [9] is considered for the design. First, the dynamics of throttle and brake, which cannot be activated simultaneously, are integrated in one state-equation model by introducing binary integer variables. Then the goal of minimizing the switching between throttle and brake, together with the safe car-following requirements and vehicle capabilities are modeled as the control objectives and constraints of ACC, respectively. The controller design is transformed to be an online mixed integer quadratic programming (MIQP), which is solved by the developed nested two-loop method. By simulating five representative traffic scenarios, it is proved that the proposed ACC algorithm provides safe vehicle following, and meanwhile reduces switching between throttle and brake, therefore improves driving comfort and fuel efficiency compared to the traditional algorithm.

The reminder of this paper is organized as follows: Section 2 is the modeling of ACC system, in which the binary integer variables are introduced to integrate the throttle and brake dynamics. Section 3 represents the controller design of ACC, in which the switching between throttle and brake is fully considered and optimized. In Section 4, the proposed optimal switching algorithm and the traditional threshold switching algorithm are simulated and analyzed in various traffic situations. The conclusion is represented in the Section 5.

2 ACC system modeling

For ACC vehicle, Song' longitudinal vehicle model [9] is considered, which assumes that the inertia of the engine and

Received 27 Demceber 2010; revised 19 August 2011.

This work was supported by Science & Technology Program of Shanghai Maritime University (No. 20120077).

the wheels are negligible, and the torque converter is locked up.

$$m\dot{v} = \frac{R_g}{h}T_e - \frac{T_{b,\max}}{h}\beta - k_{\text{roll}}mg - \frac{1}{2}k_{\text{air}}A\rho v^2 - mg\sin\theta, \tag{1}$$

where m denotes the vehicle mass, v refers to the vehicle velocity, R_g represents the effective gear ratio, T_e refers to the engine torque, h is the effective wheel radius, $T_{b,\max}$ denotes the maximum braking torque, β refers to the brake pedal position [%], k_{roll} is the rolling resistance coefficient, g represents the acceleration of gravity, k_{air} denotes the aerodynamic drag coefficient, A refers to the front area of vehicle, ρ represents the air density, and θ is the road grade.

For the throttle characteristics, the desired throttle angle can be calculated as follows [8]:

$$\alpha = TC^{-1}\Big[\frac{\dot{m}_{a0}(w_e, P_{md})}{\text{MAX}\cdot\text{PRI}(P_m/P_a)}\Big], \tag{2}$$

where α refers to the throttle angle, TC refers to the empirical throttle characteristics, m_{a0} represents the mass air flow rate into the combustion chamber, w_e refers to the engine speed, P_{md} is a nonlinear relationship between α and w_e that can be found from the table lookup map, MAX refers to a constant dependent on the size of the throttle body, PRI is the pressure influence function, P_m represents the pressure in intake manifold, and P_a refers to the atmosphere pressure.

Generally, the throttle angle is regarded as the throttle input for the vehicle, but since the engine model equation (2) depends on many factors and is often expressed in the form of empirical map, the corresponding characteristics are not considered in this paper, and the engine torque T_e is considered as the controller input instead in this design. Therefore, the control input for an ACC vehicle is given by the engine torque T_e for throttle, and the brake pedal position β for brake in this paper.

In fact, equation (1) is composed of two models (throttle and brake), since the throttle and brake actuators cannot be activated simultaneously. Two binary integer variables, ζ_1 and ζ_2, are introduced, which refer to the states of the throttle and brake actuators, respectively. Then the vehicle model can be rewritten.

$$m\dot{v} = \frac{R_g}{h}\zeta_1 T_e - \frac{T_{b,\max}}{h}\zeta_2\beta - k_{\text{roll}}mg - \frac{1}{2}k_{\text{air}}A\rho v^2 - mg\sin\theta, \tag{3}$$

$$\text{s.t.}\begin{cases}\zeta_1 \in \{0,1\},\\ \zeta_2 \in \{0,1\},\\ \zeta_1+\zeta_2 \leqslant 1,\end{cases} \tag{4}$$

where the binary integer '0' refers to the disabled state, and '1' refers to the enabled state. The constraint $\zeta_1+\zeta_2 \leqslant 1$ represents that the throttle and brake cannot be enabled at the same time.

For ACC system, the state vector $\boldsymbol{x}$ is defined to consist of the inter-distance d, relative velocity v_r, and velocity of ACC vehicle v: $\boldsymbol{x} \triangleq [d \ \ v_r \ \ v]^T$, where the relative velocity refers to the difference between the velocity of the preceding vehicle v_p and that of ACC vehicle v.

$$v_r \triangleq v_p - v.$$

In this paper, the acceleration of the preceding vehicle a_p is modeled as the disturbance w, and the road grade is considered as zero for a nominal case, then the discrete state-space equations for the ACC system can be derived.

$$\boldsymbol{x}(k+1) = \boldsymbol{x}(k) + \boldsymbol{B}_1\zeta_1(k)u_1(k) + \boldsymbol{B}_2\zeta_2(k)u_2(k) + \boldsymbol{G}w(k) + \boldsymbol{H}, \tag{5}$$

$$\text{s.t.}\begin{cases}\zeta_1(k) \in \{0,1\},\\ \zeta_2(k) \in \{0,1\},\\ \zeta_1(k)+\zeta_2(k) \leqslant 1,\end{cases} \tag{6}$$

with

$$w(k) \triangleq a_p(k),\ \ u_1(k) \triangleq T_e(k),\ \ u_2(k) \triangleq \beta(k),$$

$$f(\boldsymbol{x}(k)) = \begin{bmatrix} x_1(k) + T_s x_2(k) + 0.5c_4T_s x_3^2(k)\\ x_2(k) + c_4 T_s x_3^2(k)\\ x_3(k) - c_4T_s x_3^2(k)\end{bmatrix},$$

$$\boldsymbol{B}_1 = \begin{bmatrix}-0.5c_1T_s^2\\ -c_1T_s\\ c_1T_s\end{bmatrix},\ \ \boldsymbol{B}_2 = \begin{bmatrix}0.5c_2T_s^2\\ c_2T_s\\ -c_2T_s\end{bmatrix},$$

$$\boldsymbol{G} = \begin{bmatrix}0.5T_s^2\\ T_s\\ 0\end{bmatrix},\ \ \boldsymbol{H} = \begin{bmatrix}0.5c_3T_s^2\\ c_3T_s\\ -c_3T_s\end{bmatrix},$$

where T_s represents the sampling period of discrete ACC system, $u_1(k)$ and $u_2(k)$ refers to the two control inputs of throttle and brake actuators, respectively, and the parameters c_1, c_2, c_3, c_4 are defined as follows:

$$c_1 \triangleq \frac{R_g}{mh},\ \ c_2 \triangleq \frac{T_{b,\max}}{mh},\ \ c_3 \triangleq \frac{k_{\text{air}}A\rho}{2m},\ \ c_4 \triangleq k_{\text{roll}}\text{g}.$$

3 Controller design

In this section, the optimal switching between throttle and brake is considered in the procedure of ACC design. The objectives of minimizing the switching between throttle and brake, together with the requirements of safe car following and vehicle capabilities are modeled as the control objectives and constraints in MPC framework, and then the controller design is transformed to be an online constrained optimal control problem.

In vehicle following control, the ACC vehicle regulates the vehicle speed toward the speed of the preceding vehicle, and keeps the inter-distance to the desired value.

$$\text{Objectives}: \begin{cases}\delta(k) \to 0\\ v_r(k) \to 0\end{cases} \text{as } k \to \infty, \tag{7}$$

with $\delta(k) \triangleq d(k) - d_{\text{des}}(k)$, $d_{\text{des}}(k) = d_0 + t_h v(k)$, where δ refers to the spacing error between the actual inter-distance and the desired value, d_{des} refers to the desired following distance and constant time headway policy [10] is utilized here, d_0 represents the fix distance, and t_h represents the desired time headway.

During the car following process, the inter-distance between the ACC vehicle and its preceding one should be larger than a minimum value $d_{\min}$ to avoid collisions.

$$\text{Constraints}: d(k) \geqslant d_{\min}. \tag{8}$$

Moreover, the absolute value of acceleration is minimized [11] to provide comfortable driving to passengers.

$$\text{Objectives}: \min|a(k)|. \tag{9}$$

Considering the vehicle capabilities, the velocity, acceleration, control commands of the throttle and brake should be constrained:

$$\text{Constraints}: v_{\min} \leqslant v(k) \leqslant v_{\max}, \tag{10}$$

$$\text{Constraints}: a_{\min} \leqslant a(k) \leqslant a_{\max}, \tag{11}$$

$$\text{Constraints}: u_{1,\min} \leqslant u_1(k) \leqslant u_{1,\max}, \tag{12}$$

$$\text{Constraints}: u_{2,\min} \leqslant u_2(k) \leqslant u_{2,\max}. \tag{13}$$

After satisfying the above requirements and vehicle abilities of ACC, we minimize the switching times between throttle and brake in the control process, in order to avoid frequent switching, improve driving comfort and fuel economy. This requires that the state value of the throttle or brake should remain as constant as possible, which yields:

$$\text{Objectives}: \begin{cases} \min|\zeta_1(k+1)-\zeta_1(k)|, \\ \min|\zeta_2(k+1)-\zeta_2(k)|. \end{cases} \tag{14}$$

Therefore, the control objectives of ACC have been modeled respectively, and then we define the performance vector y as follows: $\boldsymbol{y}(k) \triangleq [\delta(k)\ \ v_{\rm r}(k)\ \ a(k)]^{\rm T}$.

Its relationship with the state vector $\boldsymbol{x}$ can be derived.

$$\boldsymbol{y}(k) = g(\boldsymbol{x}(k)) + \boldsymbol{D}_1\zeta_1(k)u_1(k) + \boldsymbol{D}_2\zeta_2(k)u_2(k) + \boldsymbol{Z}, \tag{15}$$

with

$$g(\boldsymbol{x}(k)) = \begin{bmatrix} x_1(k) + t_{\rm h}x_3(k) \\ x_2(k) \\ -c_4x_3^2(k) \end{bmatrix},\ \boldsymbol{D}_1 = \begin{bmatrix} 0 \\ 0 \\ c_1 \end{bmatrix},$$

$$\boldsymbol{D}_2 = \begin{bmatrix} 0 \\ 0 \\ -c_2 \end{bmatrix},\ \boldsymbol{Z} = \begin{bmatrix} 0 \\ 0 \\ -c_3 \end{bmatrix}.$$

The basic of the MPC principle is that the control law is obtained by solving a constrained finite-horizon optimal control problem over a predictive horizon. It has advantages in handling constraints, multiple control objectives, model mismatch and etc. [12].

It can be seen that the prediction model, equations (5)–(6) and (15) are nonlinear. For convenience, we linearize the nonlinear components around the current operating point with its tangent at each sampling instant [13]. This gives the following linear prediction model:

$$\boldsymbol{x}(k+1) = \boldsymbol{A}_{\rm r}(\boldsymbol{x}(k))\mathrm{x}(k) + \boldsymbol{B}_1\zeta_1(k)u_1(k) + \boldsymbol{B}_2\zeta_2(k)u_2(k) + \boldsymbol{G}w(k) + \boldsymbol{H}_{\rm r}(\boldsymbol{x}(k)), \tag{16}$$

$$\boldsymbol{y}(k) = \boldsymbol{C}_{\rm r}(\boldsymbol{x}(k)) + \boldsymbol{D}_1\zeta_1(k)u_1(k) + \boldsymbol{D}_2\zeta_2(k)u_2(k) + \boldsymbol{Z}_{\rm r}(\boldsymbol{x}(k)), \tag{17}$$

where

$$\boldsymbol{A}_{\rm r} = \begin{bmatrix} 1 & T_{\rm s} & c_4T_{\rm s}^2x_3|_k \\ 0 & 1 & 2c_4T_{\rm s}x_3|_k \\ 0 & 1 & 1-2c_4T_{\rm s}x_3|_k \end{bmatrix},$$

$$\boldsymbol{H}_{\rm r} = \begin{bmatrix} 0.5c_3T_{\rm s}^2 - 0.5c_4T_{\rm s}^2x_3|_k^2 \\ c_3T_{\rm s} - c_4T_{\rm s}x_3|_k^2 \\ -c_3T_{\rm s} + c_4T_{\rm s}x_3|_k^2 \end{bmatrix},$$

$$\boldsymbol{C}_{\rm r} = \begin{bmatrix} 1 & 0 & -t_{\rm h} \\ 0 & 1 & 0 \\ 0 & 1 & -c_4T_{\rm s}x_3|_k^2 \end{bmatrix},\ \boldsymbol{Z}_{\rm r} = \begin{bmatrix} -d_0 \\ 0 \\ -c_3 + c_4x_3|_k^2 \end{bmatrix},$$

where $x_3|_k$ represents the value of the state variable x_3 at the sampling instant k.

In the MPC framework, the performance criterion of ACC is obtained by synthesizing the control objectives into the following quadratic form:

$$\begin{aligned} J = & \sum_{i=1}^{N_{\rm p}}[(\hat{\boldsymbol{y}}_{\rm p}(k+i) - \boldsymbol{y}_{\rm ref}(k+i))^{\rm T}\boldsymbol{Q}(\hat{\boldsymbol{y}}_{\rm p}(k+i) \\ & -\boldsymbol{y}_{\rm ref}(k+i))] + \sum_{i=0}^{N_{\rm m}-1}u_1(k+i)^{\rm T}R_1u_1(k+i) \\ & + \sum_{i=0}^{N_{\rm m}-1}u_2(k+i)^{\rm T}R_2u_2(k+i) \\ & + \sum_{i=0}^{N_{\rm m}-2}\zeta_1(k+i)^{\rm T}S_1\zeta_1(k+i) \\ & + \sum_{i=0}^{N_{\rm m}-2}\zeta_2(k+i)^{\rm T}S_2\zeta_2(k+i), \end{aligned} \tag{18}$$

where $N_{\rm p}$ and $N_{\rm m}$ refer to the predictive horizon and control horizon respectively, $\hat{y}_{\rm p}$ refers to the predictive performance vector, $\boldsymbol{y}_{\rm ref}$ represents the reference trajectory for the performance vector, $\boldsymbol{Q}$ refers to the weighting matrix for the performance vector, R_1, R_2, S_1 and S_2 are the weighting coefficients regarding the control command and the switching respectively.

The constraints of ACC represented by equations (6), (8), (10)–(13) are integrated in the following form:

$$\begin{cases} \boldsymbol{M} \leqslant \boldsymbol{E}_{\rm r}\boldsymbol{x}(k) + \boldsymbol{D}_1\zeta_1(k)u_1(k) \\ \qquad + \boldsymbol{D}_2\zeta_2(k)u_2(k) + \boldsymbol{F}_{\rm r} \leqslant \boldsymbol{N}, \\ u_{1,\min} \leqslant u_1(k) \leqslant u_{1,\max},\ u_{2,\min} \leqslant u_2(k) \leqslant u_{2,\max}, \\ \zeta_1(k) \in \{0,1\},\ \zeta_2(k) \in \{0,1\},\ \zeta_1(k) + \zeta_2(k) \leqslant 1, \end{cases} \tag{19}$$

with

$$\boldsymbol{E}_{\rm r} = \begin{bmatrix} 1 & 0 & 0 \\ 0 & 0 & 1 \\ 0 & 0 & -2c_4x_3|_k \end{bmatrix},\ \boldsymbol{M} = \begin{bmatrix} d_{\min} \\ v_{\min} \\ a_{\min} \end{bmatrix},$$

$$\boldsymbol{F}_{\rm r} = \begin{bmatrix} 0 \\ 0 \\ -c_3 + c_4x_3|_k^2 \end{bmatrix},\ \boldsymbol{N} = \begin{bmatrix} \mathrm{Inf} \\ v_{\max} \\ a_{\max} \end{bmatrix},$$

where Inf represents a real positive infinite value, indicating that the inter-distance has no upper bound.

Then the control command $u_1(k)$ and $u_2(k)$ are solved by minimizing the equation (18) restricted by equation (19). It can be transformed to be an online mixed integer quadratic programming (MIQP), which includes both the continuous variables $u_1(k), u_1(k+1), \dots, u_1(k+N_{\rm m}-1)$, $u_2(k)$, $u_2(k+1), \dots, u_2(k+N_{\rm m}$-1) and the binary integer variables $\zeta_1(k), \zeta_1(k+1), \dots, \zeta_1(k+N_{\rm m}-1)$, $\zeta_2(k)$, $\zeta_2(k+1), \dots, \zeta_2(k+N_{\rm m}-1)$.

In order to solve MIQP, a two-loop nested method [14] is developed. In the outer loop, we use particle swarm optimization (PSO) method [15–16] for the integer optimization. Given the integer variables by the outer loop, it is referred to as a quadratic program (QP) in the inner loop, which can be solved by the mathematical programming solver [17]. Then the inner solution is returned to the outer loop to generate a new solution for the next iteration. This procedure continues until the termination criterion is satisfied. The nested solving method decomposes the MIQP into an integer optimization and a QP problem, thus simplifies the original problem, in regard to both the complexity and dimension.

By solving the online MIQP at each sampling instant, the control sequences regarding the throttle and brake are obtained, the corresponding actuator is activated and only the first command is applied to the ACC system.

4 Simulation and discussion

The objective of this section is to evaluate the performance of the proposed ACC algorithm. Five representative traffic scenarios are simulated, which includes following the preceding vehicle with varying speed, approaching, cut in, cut out and hard stop, as Fig. 1 represents. For each traffic scenario, the proposed optimal switching ACC algorithm (ACC–optimal) and the traditional algorithm with threshold switching criterion (ACC–former) are simulated, and the corresponding responses are analyzed and compared. The switching times between throttle and brake are used to evaluate the switching performance, as Table 1 represents. The mean values of absolute acceleration and jerk are collected and regarded as the comfort metrics [11]. The comprehensive modal emissions model (CMEM) [18] developed at the University of California (UC), Riverside, is used to calculate the fuel consumption. The comparison results of two algorithms are represented in Table 2.

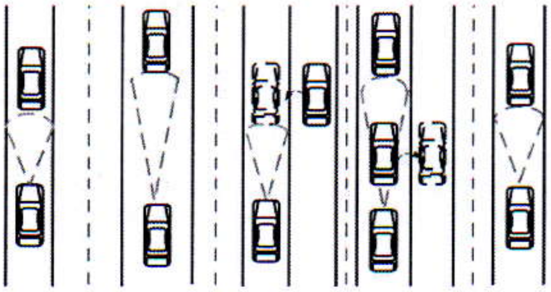

(a) Following (b) Approaching (c) Cutin (d) Cutout (e) Hard stop

Fig. 1 Five representative traffic scenarios in ACC.

Table 1 Switching times between throttle and brake of two algorithms.

Switching times	Scenario 1	Scenario 2	Scenario 3	Scenario 4	Scenario 5
ACC–former	4	2	2	2	1
ACC–optimal	2	0	0	0	1

Table 2 Improvements regarding comfort metrics and fuel consumption by comparing ACC–optimal to ACC–former.

%

Improvements	Scenario 1	Scenario 2	Scenario 3	Scenario 4	Scenario 5
Mean acceleration	6.27	23.86	15.25	26.59	10.59
Mean jerk	22.18	21.83	25.41	23.48	19.95
Fuel consumption	8.02	5.76	2.42	11.47	8.15

An encounter traffic condition is considered feasible if the ACC vehicle can change from its current velocity to that of the preceding vehicle, and meanwhile avoid a collision. In case an infeasible state is encountered, ACC vehicle is unable to prevent a collision, and then drivers must intervene and perform the effective maneuver. As we are concerned with the performance of the proposed ACC algorithm, the initial states are guaranteed feasible [19].

The parameters for ACC system are as follows [9]:

$$R_g = 3.77,\ \ h = 0.318\,\mathrm{m},\ \ m = 1620\,\mathrm{kg},$$
$$T_{\mathrm{b,max}} = 4093\,\mathrm{Nm},\ \ k_{\mathrm{air}} = 0.285,\ \ \rho = 1.23\,\mathrm{N/m^2},$$
$$k_{\mathrm{roll}} = 0.015,\ \ A = 2.2\,\mathrm{m^2},\ \ \mathrm{g} = 9.8\,\mathrm{N/m^2},$$
$$T_s = 0.2\,\mathrm{s},\ \ t_h = 1\,\mathrm{s},\ \ \tau = 0.5\,\mathrm{s},\ \ d_0 = 7\,\mathrm{m},$$
$$d_{\min} = 5\,\mathrm{m},\ \ v_{\min} = 0\,\mathrm{m/s},\ \ v_{\max} = 40\,\mathrm{m/s},$$
$$u_{1,\min} = 0\,\mathrm{Nm},\ \ u_{1,\max} = 0.36\,\mathrm{k}\cdot\mathrm{Nm},\ \ u_{2,\min} = 0,$$
$$u_{2,\max} = 1,\ \ a_{\min} = -5.5\,\mathrm{m/s^2},\ \ a_{\max} = 2.5\mathrm{m/s^2}.$$

Scenario 1 following the preceding vehicle with varying speed.

In this scenario, the ACC–equipped vehicle is following the preceding vehicle with varying speed. Fig. 2 represents the responses of ACC–optimal and ACC–former. It can be seen that both the two algorithms regulate the speed and inter-distance to adapt the variation of preceding vehicle. Safety is guaranteed (collision is avoided), and car following behavior is satisfied in two algorithms. According to Fig. 2 (d), ACC–former activates throttle actuator at first, and performs a large engine input to following the preceding vehicle. Then ACC–former switches to the brake actuator to adapt the decreasing behavior of preceding vehicle. At $t = 6\,\mathrm{s}$, the preceding vehicle begins to accelerate, which causes that the actuator is switched to the throttle actuator again. Due to the rapid decreasing of inter-distance (Fig. 2 (a)), ACC–former switches to the brake actuator at $t = 12.2\,\mathrm{s}$ to prevent collision. With the frequent speed change of preceding vehicle, it has been switched between throttle and brake actuators four times in this scenario (Table 1). While the proposed optimal ACC algorithm optimizes the switching properties, behaves smoother in velocity and acceleration responses (Figs. 2 (b)–2 (c)), and this is beneficial to service lives of vehicle mechanical components. Compared to ACC–former, the switching times in ACC–optimal between throttle and brake is decreased to be 2. Moreover, driving comfort and fuel-economy are improved in ACC–optimal, since the mean values of absolute acceleration and jerk (comfort metrics) are decreased by 6.27% and 22.18% respectively, and the fuel consumption is reduced by 8.02% (Table 2).

Scenario 2 Approaching.

In this scenario, the ACC–equipped vehicle approaches a preceding vehicle from a large inter-distance. The responses of ACC–optimal and ACC–former are represented in Fig. 3. According to Fig. 3, ACC–former implements a large engine input initially, and maintains it for seconds to approach the preceding vehicle quickly. The corresponding velocity achieves to nearly 22 m/s. Due to the larger velocity, the inter-distance is decreased in a short time, and collisions may occur if it continues accelerating. So ACC–former switches to the brake actuator swiftly, and takes a sudden brake. At $t = 5$ s, the preceding vehicle begins to accelerate, ACC–former has to switch to the throttle actuator again to adapt this speed variation. It can be seen that the switching between throttle and brake is not considered and optimized in ACC–former, so ACC–former accelerates intensely at first and brakes suddenly afterwards, which causes frequent switching (Table 1). However, ACC–optimal behaves smoother and avoids the switching between throttle and brake. In the beginning of the approaching process, ACC–optimal performs smooth acceleration, and decreases the throttle input (releases the throttle pedal) gradually. The velocity achieves to about 19 m/s. Therefore, it is not necessary to switch to the brake actuator when the inter-distance is regulated to the small value. Without switching between throttle and brake, ACC–optimal improves driving comfort significantly, because the comfort metrics, the mean absolute values of acceleration and jerk are reduced by 23.86% and 21.83% than the formal algorithm (Table 2). Moreover, the fuel consumption is saved by 5.76% in ACC–optimal, which indicates that fuel efficiency is increased.

Scenario 3 Cut in.

In this scenario, the ACC–equipped vehicle is running in the steady state with a constant speed initially, and a vehicle from another lane performs cut in at $t = 5$ s. Fig. 4 represents the responses of ACC–former and ACC–optimal. It can be seen that both the two algorithms perform similar velocity profiles in this situation, since no matter what kind of ACC algorithm is adopted, the control objectives are to avoid collisions when cut in occurs, and meanwhile regulate velocity and spacing to adapt the variation of the preceding vehicle. However, there is a main difference in the control profile between two algorithms. At the initial moment of cut in, the inter-distance is decreased instantaneously, ACC–former activates the brake actuator. When the accelerating behavior of the preceding vehicle is realized, ACC–fomer switches to the throttle actuator promptly. While ACC–optimal balances the successive actions of braking and accelerating effectively, and optimizes the switching behavior. Only the throttle actuator is activated in the whole driving process, and the switching is avoided. According to Table 2, ACC–optimal provides smaller acceleration and jerk, and decreases fuel consumption, which will increase human drivers' satisfaction. Though the responses of two algorithms are a little similar in this scenario, the proposed ACC new algorithms will be more acceptable since it can decrease the switching times, improve driving comfort and fuel efficiency.

Scenario 4 Cut out.

In this scenario, the ACC–equipped vehicle follows the preceding vehicle with a constant speed initially. At $t = 5$ s, the preceding vehicle performs a cut out suddenly, which causes the ACC–equipped vehicle follows a new preceding vehicle in the same lane. The corresponding responses are represented in Fig. 5. It can be seen that the initial steady state is interrupted and the inter-distance is increased instantaneously due to the cut out. In order to get close to the new preceding vehicle as soon as possible, ACC–former activates throttle actuator and performs a large engine input. The corresponding velocity increases from 15 m/s to 21.66 m/s in three seconds. With the rapid decreasing of inter-distance, ACC–former switches to the brake actuator soon afterwards, in order to avoid possible collisions. According to Table 1, it has been switched between throttle and brake twice in this scenario. However, ACC–optimal performs smooth acceleration in the whole process. The switching performance is fully considered in ACC–optimal, and the frequent switching between throttle and brake is prevented. Compared to ACC–former, driving comfort is improved in ACC–optimal, since the magnitudes of acceleration and jerk (comfort metrics) is decreased by 26.59% and 23.48%, respectively. Moreover, ACC–optimal reduces the fuel consumption by 11.47% than ACC–former (Table 2).

Scenario 5 Hard stop.

This traffic scenario depicts the situation where the preceding vehicle takes a hard stop, and the corresponding responses of two ACC algorithms are shown in Fig. 6. In this scenario, both the two algorithms switch to the brake actuator from the throttle actuator, and take a large brake input to prevent collisions (Fig. 6 (d)). It can be seen that the superiority of ACC–optimal in switching performance is not obvious (Table 1). This is because safety is regarded as the top priority of ACC algorithms, and ACC–equipped vehicle should take suitable brake actions when the preceding vehicle performs hard stop, no matter what kind of ACC algorithm is adopted. Therefore, the switching between different actuators could not be prevented in this scenario. Despite of this, the proposed optimal switching ACC algorithms behaves better performance in driving comfort and fuel-economy than ACC–former, as Table 2 represents.

Above all, the simulation results show that the proposed ACC algorithm guarantees safe car following, outperforms the traditional algorithms by avoiding the frequent switching between throttle and brake, and meanwhile increases driving comfort and fuel efficiency significantly.

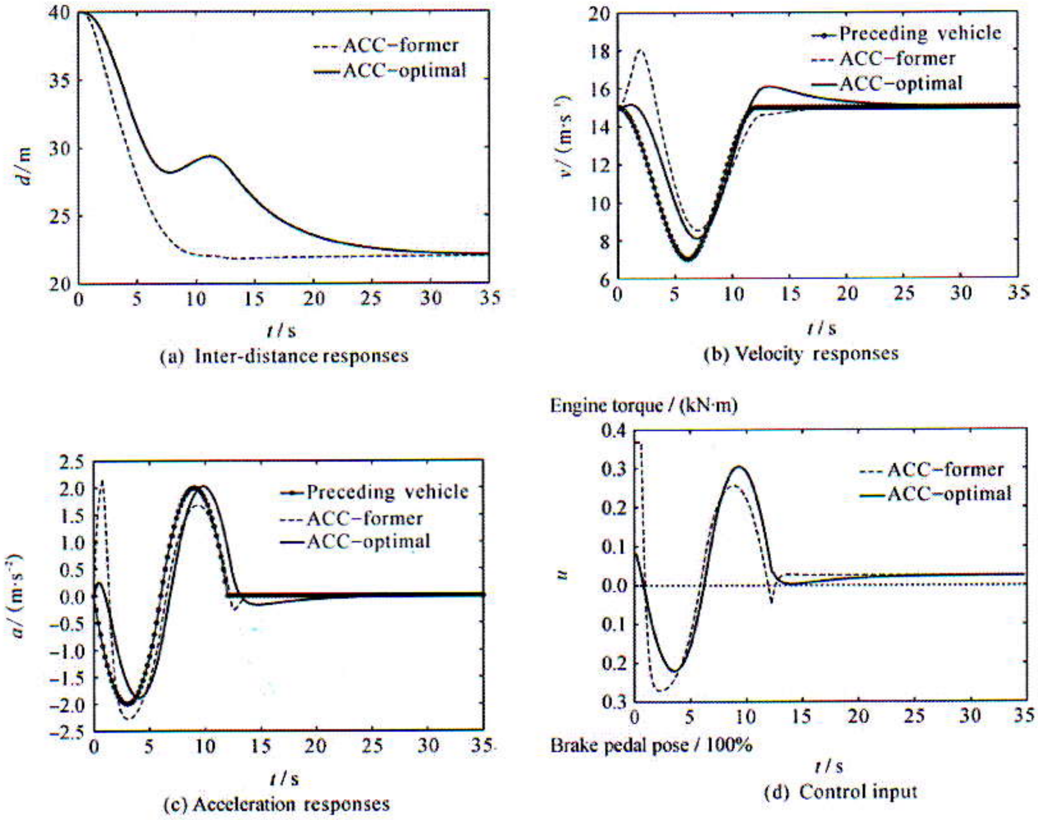

Fig. 2 Responses of ACC–optimal and ACC–former in the scenario of following the preceding vehicle with varying speed.

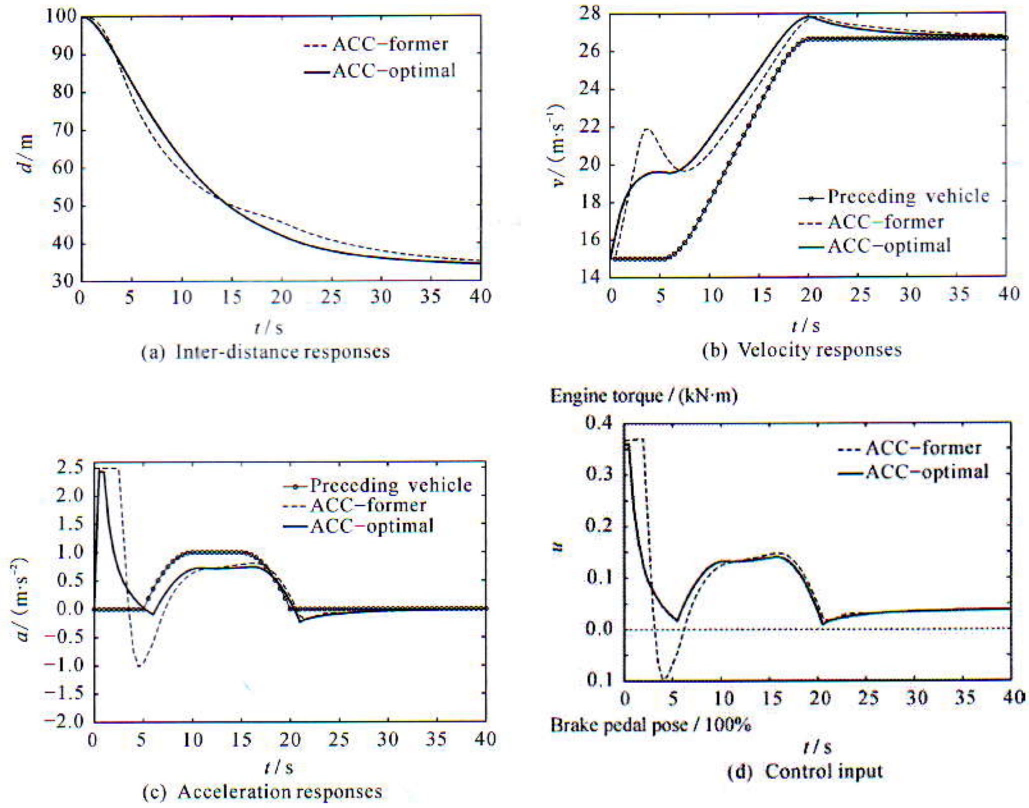

Fig. 3 Responses of ACC–optimal and ACC–former in the scenario of approaching.

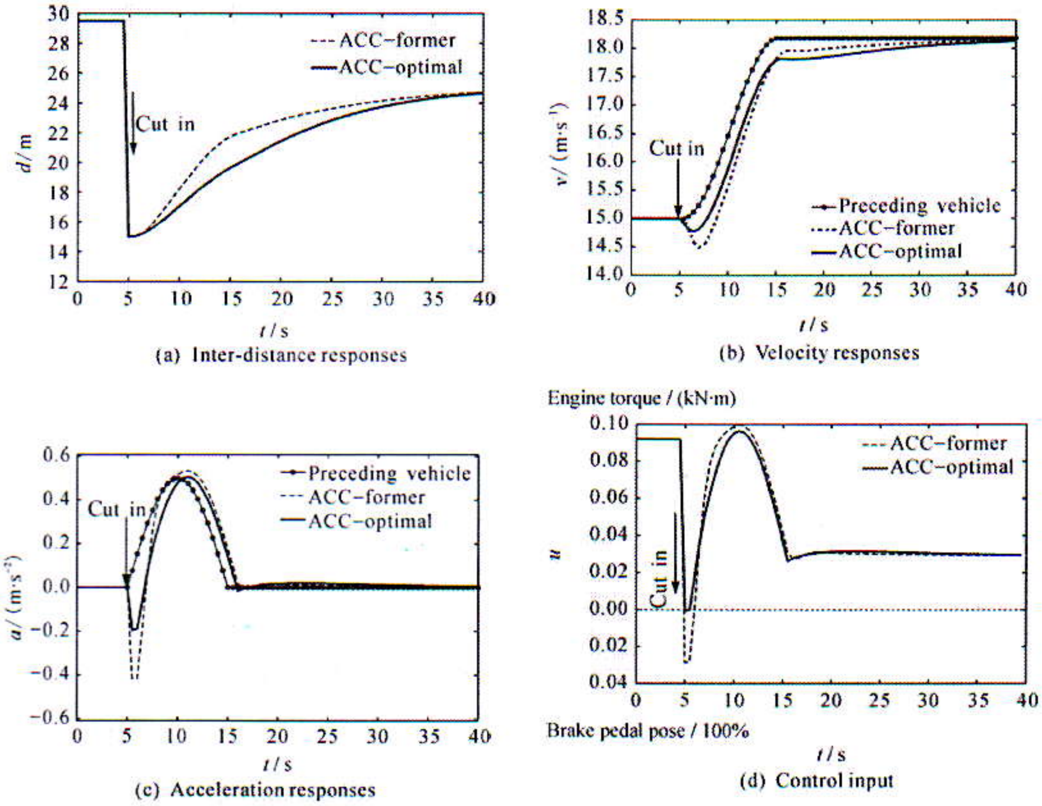

(a) Inter-distance responses (b) Velocity responses

(c) Acceleration responses (d) Control input

Fig. 4 Responses of ACC–optimal and ACC–former in the scenario of cut in.

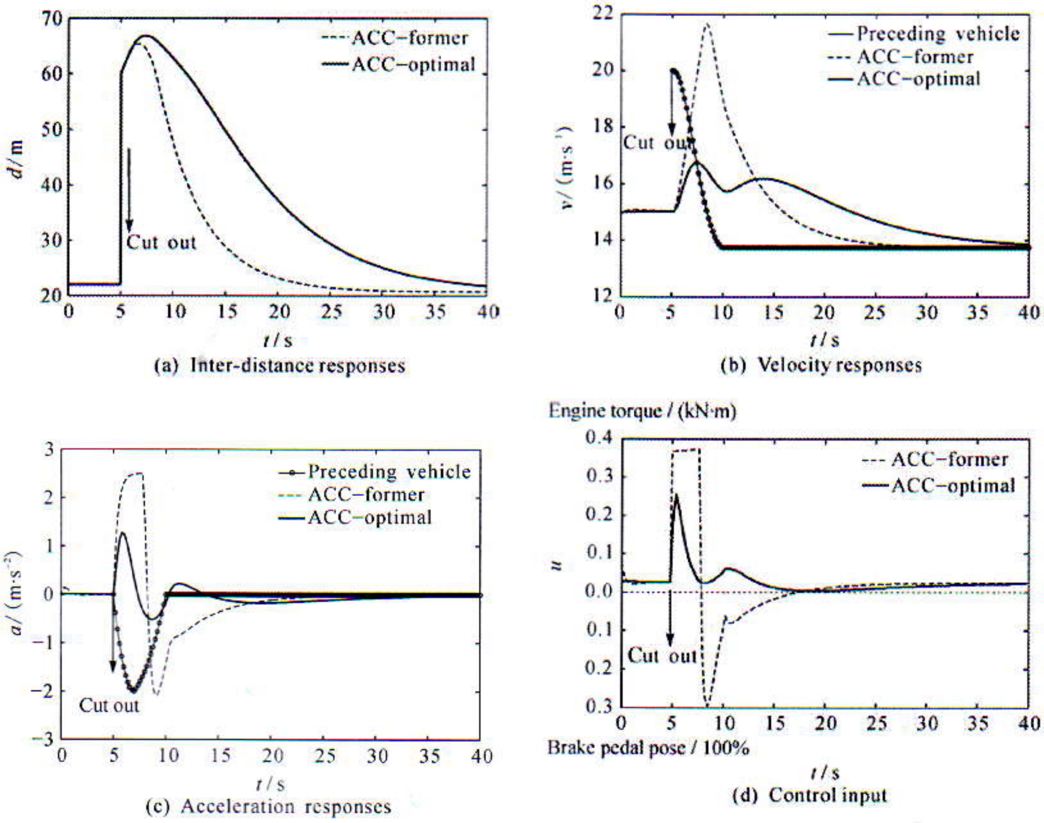

(a) Inter-distance responses (b) Velocity responses

(c) Acceleration responses (d) Control input

Fig. 5 Responses of ACC–optimal and ACC–former in the scenario of cut out.

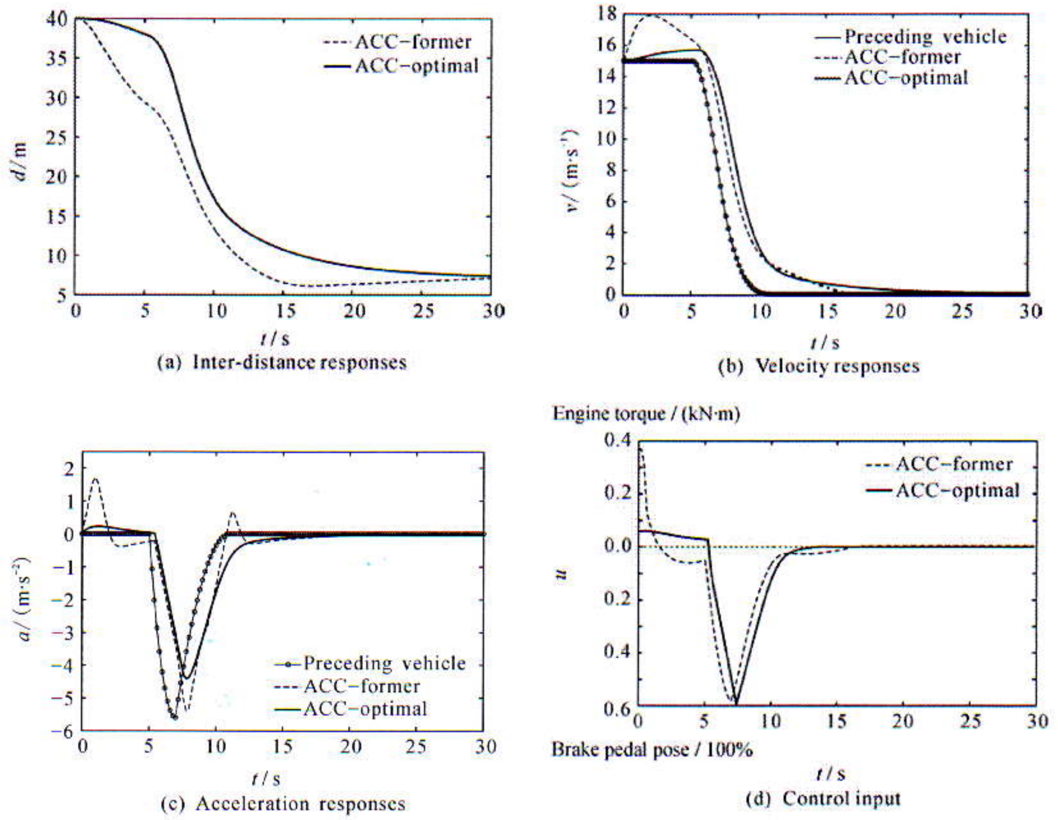

Fig. 6 Responses of ACC–optimal and ACC–former in the scenario of hard stop.

5 Conclusion

In this paper, an ACC algorithm with the optimal switching between throttle and brake was proposed in MPC framework. Since the throttle and brake cannot be activated simultaneously, the integer variables are introduced to integrate their dynamics in one model. Then the control objectives and requirements of ACC are modeled respectively, and the controller design is transformed to be an online constrained optimal control problem. By simulating the representative traffic scenarios, it was proved that the proposed ACC algorithm can effectively optimize the successive accelerating and braking behavior, and avoids frequent switching between throttle and brake actuators. Compared to the traditional ACC algorithms, the proposed one not only meets the safe car following, but also behaves smoother performances, decreases the switching times, improves driving comfort, and enhances the fuel economy significantly. Therefore, the proposed ACC algorithm will be more acceptable to human drivers and lead to its increased usage in application.

References

[1] A. Vahidi, A. Eskandarian. Research advances in intelligent collision avoidance and adaptive cruise control. *IEEE Transactions on Intelligent Transportation Systems*, 2003, 4(3): 143 – 153.

[2] L. Xiao, G. Feng. A comprehensive review of development of adaptive cruise control systems. *Vehicle System Dynamics*, 2010, 48(10): 1167 – 1192.

[3] R. Rajamani. *Vehicle Dynamics and Control*. New York: Springer, 2006: 153 – 181.

[4] J. C. Gerdes, J. K. Hedrick. Vehicle speed and spacing control via coordinated throttle and brake actuation. *Control Engineer Practice*, 1997, 5(11): 1607 – 1614.

[5] Y. Zhang, E. B. Kosmatopoulos, P. A. Ioannou, et al. Autonomous intelligent cruise control using front and back information for tight vehicle following maneuvers. *IEEE Transactions on Vehicular Technology*, 1999, 48(1): 319 – 328.

[6] J. Karl Hedrick, X. Y. Lu. Heavy-duty vehicle modeling and longitudinal contro. *Vehicle System Dynamics*, 2005, 43(9): 653 – 669.

[7] P. Ioannou, Z. Xu, S. Eckert, et al. Intelligent cruise control: theory and experiment. *Proceedings of the 32nd IEEE Conference on Decision and Control*. San Antonlo: IEEE, 1993: 1885 – 1890.

[8] S. N. Huang, W. Ren. Vehicle longitudinal control using throttles and brakes. *Robotics and Autonomous Systems*, 1999, 26(4): 241 – 253.

[9] W. Beak, B. Song. Design and validation of a longitudinal via velocity and distance controller via hardware-in-the-loop simulation. *International Journal of Automotive Technology*, 2009, 10(1): 95 – 102.

[10] D. Swaroop, K. R. Rajagopal. A review of constant time headway policy for automatic vehicle following. *IEEE Intelligent Transportation Systems Conference*, 2001: 65 – 69.

[11] Y. Kyongsu, j. Chung. Nonlinear brake control for vehicle CW/CA systems. *IEEE/ASME Transactions on Mechatronics*, 2001, 6(1): 17 – 25.

[12] C. E. Garcia, D. M. Prett, M. Morari. Model predictive control theory and practice—A survey. *Automatica*, 1989, 25(3): 335 – 348.

[13] A. Beccuti, T. Geyer, M. Morari. A hybrid system approach to power systems voltage control. *Proceedings of the 44th IEEE Conference Decision Control*. Seville: IEEE, 2005: 6774 – 6779.

[14] X. Chen, Z. Li, J. Yang, et al. Nested tabu search (TS) and sequential quadratic programming (SQP) method, combined with adaptive model reformulation for heat exchanger network synthesis . *Industrial and Engineering Chemistry Research*, 2008, 47(7): 2320 – 2330.